Optical injection effects in electrically pumped semiconductor nano-laser arrays

Fan, Yuanlong; Shi, Teng; Zhang, Jing; Shore, K. Alan

Opt. Express

DOI:
10.1364/OE.525981

Published: 10/05/2024

Peer reviewed version

Research Article Vol. 32, No. 11 / 20 May 2024 / Optics Express 19361
Optics EXPRESS

Optical injection effects in electrically pumped semiconductor nano-laser arrays

YUANLONG FAN,[1,2,*] TENG SHI,[1,2] JING ZHANG,[1,2] AND K. ALAN SHORE[3,4]

[1]Hangzhou Institute of Technology, Xidian University, Hangzhou 311231, China
[2]School of Optoelectronic Engineering, Xidian University, Xi'an 710071, China
[3]School of Computer Science and Electronic Engineering, Bangor University, Bangor LL57 1UT, United Kingdom
[4]k.a.shore@bangor.ac.uk
[*]fanyuanlong@xidian.edu.cn

Abstract: A theoretical analysis is performed on the response of electrically pumped nano-laser arrays to external optical injection. The response to both continuous wave and modulated optical injection is explored. Continuous wave injection is shown to excite several varieties of dynamical behaviour in the array elements including regular dynamics and quasi-periodic behaviour. The strength of the optical injection, the frequency detuning between the injected light and the target laser, and the magnitude of the Purcell spontaneous emission enhancement factor are shown to markedly affect the dynamics. When subject to modulated optical injection, the effects of frequency detuning and optical injection strength are the focus of attention. It is shown that the elements of the array subject to modulated optical injection exhibit oscillatory behaviour over broad regimes determined by the optical injection strength and the frequency detuning.

1. Introduction

Over recent years there has been steady progress in the development of semiconductor nano-lasers [1–4]. Particular success has been achieved in the implementation of optically excited nano-lasers which have utilized a number of material platforms [5–8]. In contrast, fabrication of electrically pumped semiconductor nano-lasers has proved to be rather challenging, and thus examples of electrically pumped semiconductor nano-lasers are relatively rare [9–14]. Nevertheless, due to the practical utility of such electrically pumped nano-lasers, it is of importance to explore their behaviour theoretically to demonstrate their potential capabilities. To this end, there has been a wide range of theoretical work undertaken on electrically pumped semiconductor nano-lasers and notably offering delineations of their rich dynamical properties [15–17]. The effects of external perturbations on such dynamical properties has been a specific focus of theoretical research including: their direct current modulation characteristics [18]; their behaviour when subject to optical injection [19]; and when in receipt of both regular [20] and phase conjugate [21] optical feedback. Much of that work has concerned the dynamics of stand-alone semiconductor nano-lasers. However, interest has also been shown in the dynamical properties of mutually-coupled nano-lasers [22].

Semiconductor nano-lasers naturally lend themselves to assembly in one and two-dimensional arrays. A recent authoritative survey [23] has highlighted the potential applications of nano-laser arrays and has pioneered the analysis of their dynamics through considering two-element arrays. That work had the attraction of being related to seminal experimental results obtained with optically-pumped nano-laser arrays. Coupling between array elements can be expected to significantly influence both the static and dynamical behaviour of nano-laser arrays. The structure of the near and far-field emission would be a salient feature of the static behaviour nano-laser arrays. In [23] attention is, e.g., given to super-mode formation in two-element nano-laser

#525981 https://doi.org/10.1364/OE.525981
Journal © 2024 Received 11 Apr 2024; revised 5 May 2024; accepted 5 May 2024; published 10 May 2024

Optics EXPRESS

arrays. Motivated by that work, attention has been given recently to the dynamical behaviour of stand-alone electrically pumped nano-laser arrays [24]. Also a detailed exploration has been made of the direct current modulation response of such arrays [25]. The latter work exemplified the response of such arrays to an external electrical perturbation whilst the present contribution is directed at eliciting the behaviour of the arrays when subject to external optical injection.

In our previous work [24,25] attention was given to 3-element nano-laser arrays: a linear 3 element array and a triangular array. These configurations are considered as elementary elements of extensive one and two-dimensional nano-laser arrays respectively. In the present analysis we have confined attention to the response of three-element linear arrays when subject to various forms of external optical injection. It has been emphasized [24,25] that even with such basic arrays, capturing all their possible dynamical responses is highly challenging and hence efforts were made to identify representative examples of the dynamics. In that context it is noted that in this work an assumption is made that the nano-lasers in the array are identical. It is appreciated that this is rather a stringent assumption but it is expected that fabrication-related variations in device dimensions will not significantly amend the qualitative features of the dynamics found to arise in this configuration.

A distinguishing physical factor which strongly influences the richness of the dynamics in nano-lasers, in general, and nano-laser arrays, in particular, is the possibility of enhancement of spontaneous emission via the so-called Purcell effect. The influence of the Purcell factor on nano-laser array responses is explored in some detail here. The model for the analysis of optical injection is described in Section 2. Results for optical injection effects in nano-lasers arrays are described and interpreted in Section 3. Section 4 provides a conclusion and brief perspective on future analysis.

2. Model

Nano-laser arrays consisting of M identical nodes coupling to each other with optical injection can be described by modified forms of coupled rate equations incorporating the Purcell factor F and an enhanced spontaneous emission coupling factor β.

$$\begin{aligned}\frac{dS_j(t)}{dt} &= \frac{\Gamma F\beta N_j(t)}{\tau_n} + \Gamma g_n\left[N_j(t)-N_0\right]S_j(t) - \frac{S_j(t)}{\tau_p} \\ &\quad - \sum_{\substack{m=1\\ m\neq j}}^{M} 2k_{jm}S_m(t)\sin\left[\phi_m(t)-\phi_j(t)\right]\end{aligned} \tag{1}$$

$$\begin{aligned}\frac{d\phi_j(t)}{dt} &= \frac{\alpha}{2}\left\{\Gamma g_n\left[N_j(t)-N_0\right]-\frac{1}{\tau_p}\right\} \\ &\quad + \sum_{\substack{m=1\\ m\neq j}}^{M}\left\{\Delta\omega_{jm} + k_{jm}\frac{S_m(t)}{S_j(t)}\cos\left[\phi_m(t)-\phi_j(t)\right]\right\} \\ &\quad - \left(\omega_{inj}-\omega_j\right) - \xi_{inj}\sqrt{S_{inj}(t)/S_j(t)}\sin\left[\phi_{inj}(t)-\phi_j(t)\right]\end{aligned} \tag{2}$$

$$\frac{dN_j(t)}{dt} = \frac{I_j}{eV_a} - \frac{N_j(t)}{\tau_n}[F\beta + (1-\beta)] - g_n[N_j(t)-N_0]S_j(t) \tag{3}$$

where the subscripts 'j' and 'm' represent j_{th} and m_{th} laser respectively. t is the time. $S(t)$ is the photon density, $\phi(t)$ is the optical phase and $N(t)$ is the carrier density. $S_{inj}(t)$, $\phi_{inj}(t)$ and ω_{inj} are the photon density, the optical phase and the angular frequency of external laser injecting the array respectively. The injection rate controlling the optical injection into the slave laser is, $\xi_{inj} = (1\text{-}r)(R_{inj}/r)^{1/2}c/(2nL_{in})$, where R_{inj} is the injection parameter, $r = 0.85$ is the reflectivity of the laser [26], c is the speed of light in the free space, $n = 3.4$ is the refractive index and $L_{in} = 1.39\,\mu m$ is the nano-laser's internal cavity length [12]. Γ is the confinement factor, τ_n is the carrier life time, g_n is the differential gain, N_0 is the transparency carrier density, τ_p is the photon

Optics EXPRESS

lifetime, k is the coupling rate between the two lasers, α is the linewidth enhancement factor, $\Delta\omega$ is the frequency detuning between the two lasers, I is the injection current, e is the elementary charge, V_a is the volume of the active region. Note that unless stated otherwise, $I = 1.2I_{th}$ where I_{th} is the threshold current. Also note that $k_{jm} = k_{mj}$.

Three scenarios of nano-laser array with optical injection are considered and their corresponding

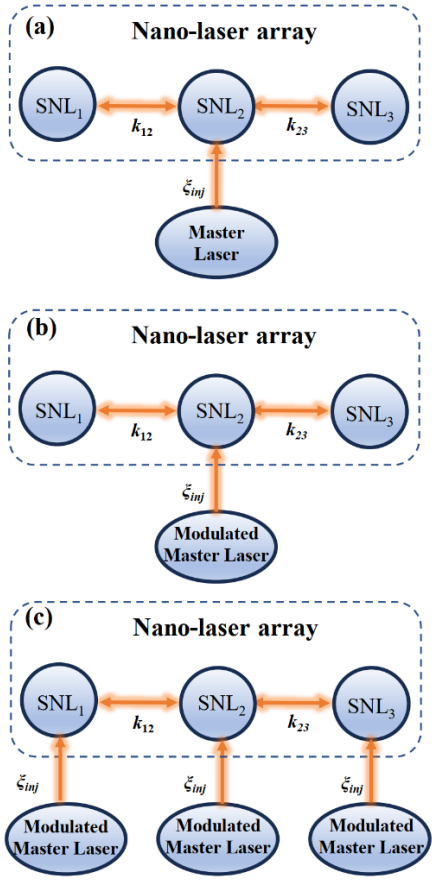

Fig. 1. Three scenarios of optical injection to the nano-laser array.

schematic diagrams are shown in Fig. 1 which can be modelled by Eqs. (1)–(3) when $M = 3$. In Fig. 1(a) we have the case of one element of the array being optically injected by a continuous wave external laser. Figure 1(b) depicts the case of a modulated external laser injecting one element of the linear array. The case shown in Fig. 1(c) is where all elements of the array are injected by modulated external lasers. Equations (1)–(3) have been solved numerically using a fourth order Runge-Kutta integration method. In the simulations, a temporal resolution of $\Delta t = 0.1$ ps is selected and the duration of the time series is set to be 1 μs. The dynamics of the nano-lasers is analysed using the device parameters given in Table 1 which are taken mainly from [12]. In an experimental investigation of optical injection, the two parameters which can be most easily accessed are the strength of the optical injection and the detuning between the master and slave lasers. As such, these parameters will be utilized in the present simulations. When consideration is given to the array response to modulated injection, consideration can be given to the modulation frequency and the depth of modulation. In the results presented here we fix

Optics EXPRESS

both those quantities as defined below. It will be appreciated that there is considerable scope for further simulations of the optical injection response of nano-laser arrays.

Table 1. Nano-laser device parameters

Symbol	Physical Meaning	Value
β	Spontaneous emission factor	0.05
Γ	confinement factor	0.65
τ_n	carrier life time	$2.00 \times 10^{-9} s$
g_n	differential gain	$1.65 \times 10^{-12} m^3/s$
N_0	carrier density at transparency	$1.10 \times 10^{24} m^{-3}$
τ_p	photon life time	$0.36 \times 10^{-12} s$
k	coupling rate	variable
α	line-width enhancement factor	variable
$\Delta\omega$	frequency detuning between adjacent slave lasers	$0\,GHz$
e	elementary charge	$1.60 \times 10^{-19} C$
V_a	volume of the active region	$3.96 \times 10^{-19} m^3$

3. Results

3.1. Continuous wave optical injection

The first outcome of the simulations shown in Fig. 2 concerns the case of Fig. 1(a) where the central element of the nano-laser array, nano-laser 2, is subject to continuous wave optical injection.

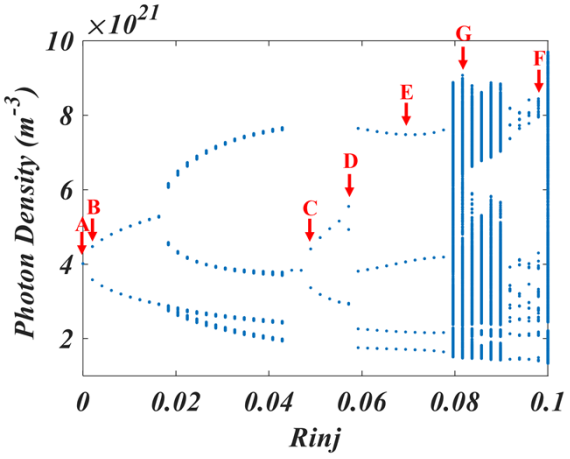

Fig. 2. The bifurcation diagram of nano-laser 2 in the first scenario of the nano-laser array with optical injection shown in Fig. 1(a) when $F = 5$, $\alpha = 5$ and $k_{12} = k_{23} = 5 \times 10^8$. The frequency detuning between the master and slave laser is $80\,GHz$.

In Fig. 2, the influence of optical injection strengths on the stability of nano-laser 2 is investigated when $F = 5$ and α=5 using bifurcation diagrams which are informative and effective means widely used for investigating the dynamics of a system as a function of one of the system parameters. The coupling rate between lasers are set to be $k_{12} = k_{23} = 5 \times 10^8$. The frequency detuning between the master and slave laser is $80\,GHz$. The bifurcation diagram is obtained by recording the local extremum of the time series of the photon density at every different point of

Optics EXPRESS

R_{inj} which takes 50 equally spaced points within the range of $R_{inj} \in [0, 0.1]$. When the nano-laser is stable (indicated A in Fig. 2), only one extremum, can be found in the temporal waveform of photon density. When the nano-laser is unstable, two or more extrema are located (indicated B-G in Fig. 2), and the number of the extrema can be used to define different types of dynamics. For example, clusters of extrema indicate quasiperiodic oscillations (indicated F in Fig. 2) whereas many extrema indicate chaos (indicated G in Fig. 2).

Figure 3 shows the corresponding time series and power spectrum of different dynamics of A-G shown in Fig. 2 which can be used to identify the transitions between those dynamics. From Fig. 3(a), it can be seen that the nano-laser is stable in the absence of optical injection. This stability can also be confirmed by the power spectrum (Fig. 3(h)) where there is a small component at around 23 GHz corresponding to the relaxation oscillation frequency of the solitary nano-laser. With increase of optical injection strength to R_{inj} =0.002, the nano-laser enters the unstable region where the photon density undergoes periodic oscillations with two local extremum (as shown in Fig. 3(b)). This dynamic reappears with a stronger optical injection strength R_{inj} =0.05 with the oscillation frequency shifts from 43 GHz (as shown in Fig. 3(j)) back to the relaxation oscillation frequency (as shown in Fig. 3(i)). Note that dynamics showing a higher oscillation frequency of 43 GHz appears when the optical injection strength is relatively small could be due to the laser enters the automodulation regime [27,28] in which the beating waveform becomes distorted. With a further increase of R_{inj}, the photon density exhibits three or four local extremum (as shown in Fig. 3(d) and (e)) which corresponding power spectra show three or four peaks (as shown in Fig. 3(k) and (l)), respectively. When the optical injection strength increases to a higher value, i.e., R_{inj} =0.08, the peaks in the spectrum are broadened and floor level increases compared to other dynamics (as shown in Fig. 3(n)). These two phenomena indicate the occurrence of chaos. Transition to quasiperiodic dynamic can be achieved by further increasing the optical injection strength, e.g., R_{inj} =0.1 where the spectrum retains many prominent peaks as shown in Fig. 3(m).

The two-dimensional (2D) maps indicate the nature of the dynamics excited in nano-laser array when subject to a range of optical injection strengths and frequency detunings between the master laser and nano-laser 2. Figure 4 summarises the differing dynamical scenarios which can be excited in nano-laser array under optical injection for several combinations of two device parameters namely the Purcell spontaneous emission enhancement factor, F, and the linewidth enhancement factor α. The interplay between these factors leads to varying admixtures of regular and quasi-periodic dynamics within the 2D portraits.

Considering the cases of α=2, it is seen that for a Purcell factor $F = 5$, dynamics with 2 local extrema is the dominant feature of the 2D portrait for the central laser. As F is increased to 10, the central laser tends to be stabilized in the negative detuning region. For the cases of α=5, several species of dynamics occupy significant areas of the portrait for the central laser. Further enhancement of the spontaneous emission with $F = 20$, dampens the system so that only 2 local extremum dynamics feature in the portrait of central laser. For the case of α=5. The damping effects of spontaneous emission enhancement are more monotonic so that for $F = 5$ several forms of dynamics are present in the portrait whereas for higher values of F the range of dynamics encountered decreases until for $F = 20$ only dynamics with 2 local extremum persists.

In Fig. 5 attention is given to the effects of continuous wave optical injection for a higher array interelement coupling strength but only for the case of α=2. Due to that higher coupling strength between the array elements, the effects of optical injection into nano-laser 2 become apparent in nano-lasers 1 and 3. As may be expected, there is a symmetry in the behaviours of nano-lasers 1 and 3. The predominant feature of the dynamics of the non-injected lasers is quasi-periodic dynamics.

Optics EXPRESS

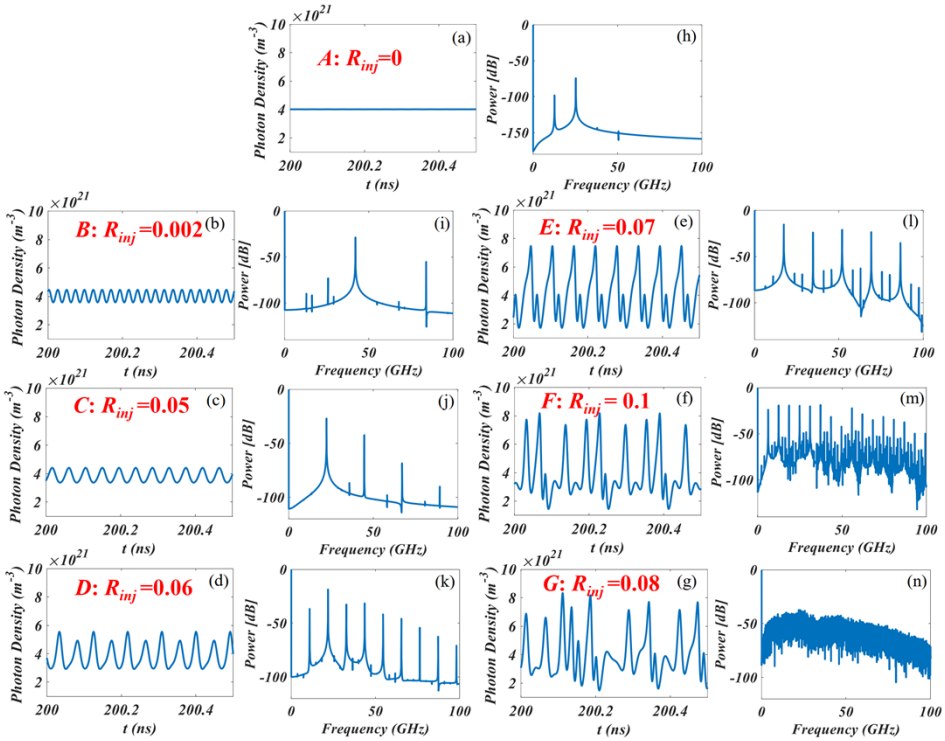

Fig. 3. Time series and power spectra for the dynamical behaviours A-G shown in Fig. 2.

3.2. *Modulated optical injection*

Consideration is now given to the arrangement shown in Fig. 1(b), namely modulated optical injection into nano-laser 2. Again, the bifurcation diagram (shown as Fig. 6) is used to identify the laser dynamics. Here the modulation frequency is fixed as 25 GHz and the modulation depth is set as 0.1. From Fig. 6, two clusters of local extremum are the dominant dynamics when the optical injection strength is less than R_{inj} =0.086, after which two local extremum becomes dominant.

Before assembling relevant 2D portraits pertinent to this case, the corresponding time-series and spectrum of the dynamics in Fig. 6 are given in Fig. 7. It is seen from Fig. 7 that as the optical injection strength is increased the predominant dynamics of the slave laser becomes locked to the modulated optical injection.

Moving now to the case shown in Fig. 5 of stronger inter-element coupling, it is shown as the optical injection strength and detuning between master and slave are changed, the oscillation frequencies induced in the central laser exhibit considerable variation, as shown in Fig. 8. The recorded oscillation frequency is the highest frequency component in the spectrum. It is noted that the symmetry of the behaviours of nano-lasers 1 and 3 is preserved where the lasers remain quiescent when the frequency detuning between −50 GHz to 50 GHz. Beyond this region, the lasers tend to show a lower oscillation frequency. Nano-laser 2 undergoes a rather more orderly progression through bands of oscillation frequencies.

Moving now to the case for a larger value of modulation depth of $m = 0.3$, it is shown in Fig. 9 that nano-lasers 1 and 3 no longer remain quiescent. Again, nano-laser 2 undergoes a rather more orderly progression through bands of oscillation frequencies and the symmetry of the behaviours

Optics EXPRESS

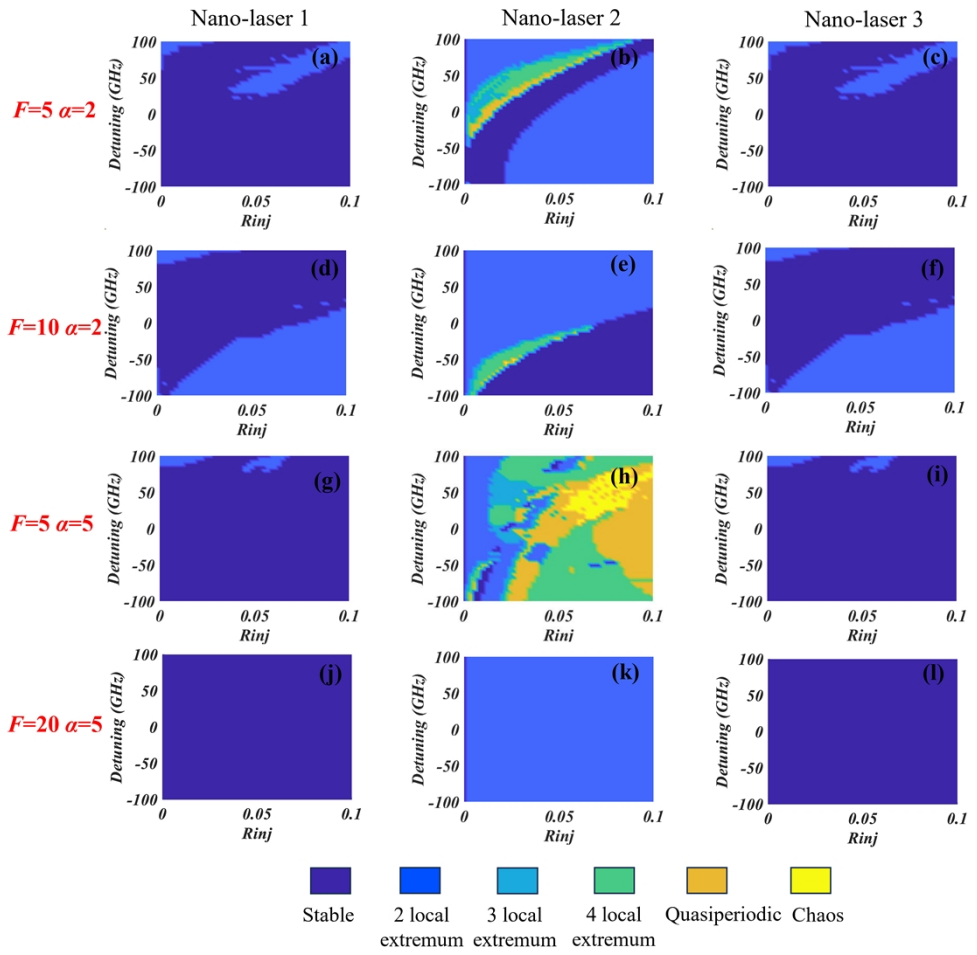

Fig. 4. 2D maps of dynamics of nano-lasers in the first scenario of the nano-laser array with optical injection shown in Fig. 1(a) when the coupling rate $k_{12} = k_{23} = 5 \times 10^8$.

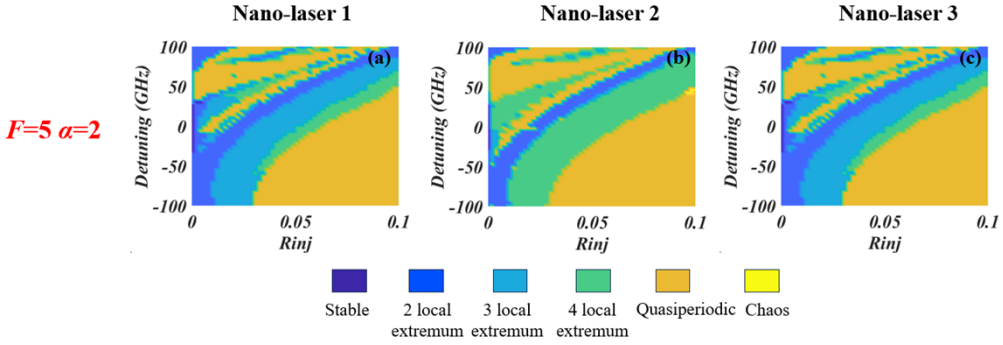

Fig. 5. 2D maps of dynamics of nano-lasers in the first scenario of the nano-laser array with optical injection shown in Fig. 1(a) when the coupling rate $k_{12} = k_{23} = 5 \times 10^9$. Note that comparing to Fig. 4, all lasers in the array shows complex dynamics in Fig. 5.

Optics EXPRESS

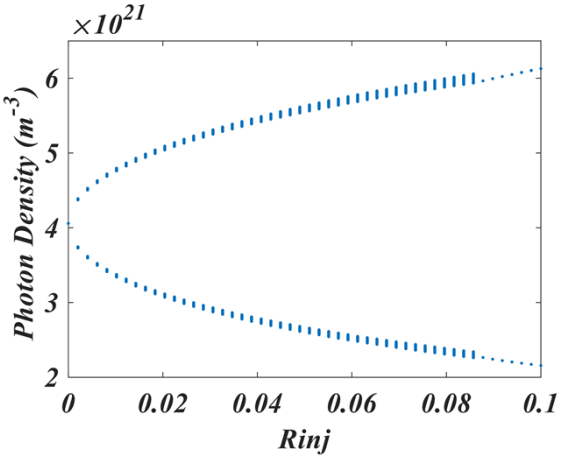

Fig. 6. The bifurcation diagram of nano-laser 2 in the second scenario of the nano-laser array with optical injection shown in Fig. 1(b) when $F = 20$, $\alpha = 2$ and $k_{12} = k_{23} = 5 \times 10^8$. The frequency detuning between the master and slave laser is $-96\,GHz$.

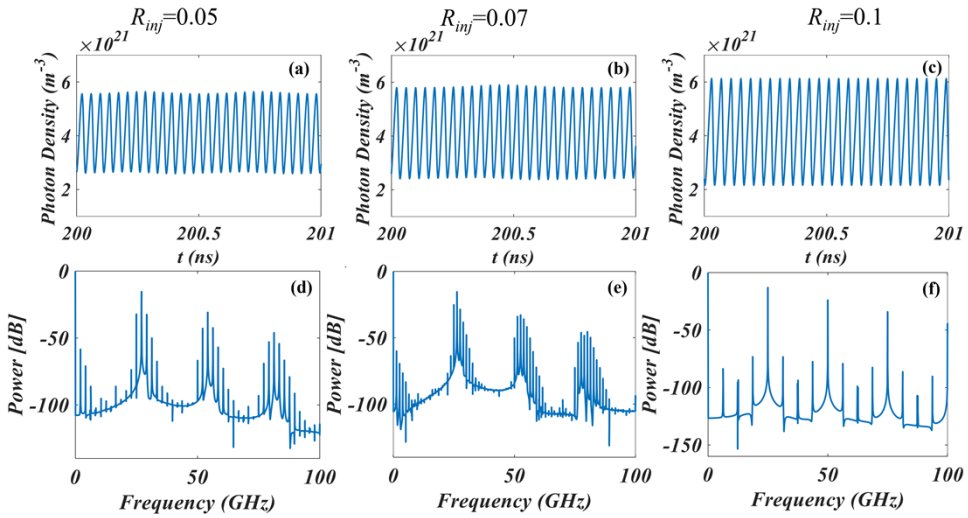

Fig. 7. Time series and the corresponding spectrum of nano-laser 2 in the second scenario of the nano-laser array with optical injection shown in Fig. 1(b) when α=2 and the coupling rate $k_{12} = k_{23} = 5 \times 10^8$. The modulation frequency and the modulation depth of the master laser are set to be 25 GHz and 0.1 respectively. Note that nano-laser 1 and 3 remains stable.

of nano-lasers 1 and 3 is preserved. These lasers tend to show lower oscillation frequencies but nevertheless show some regions of higher oscillations.

Finally, attention is given to the arrangement shown in Fig. 1(c) wherein all slave lasers are subject to modulated optical injection. In Fig. 10, all slave lasers are subjected to modulated optical injection at a frequency of 25 GHz. It is seen that the trend seen in nano-laser 2 in Fig. 9, is now shared with nano-lasers 1 and 3. That is to say a relatively orderly change through bands of higher to lower frequencies is recorded. The symmetry of behaviours of nano-lasers 1 and 3 is again apparent.

Optics EXPRESS

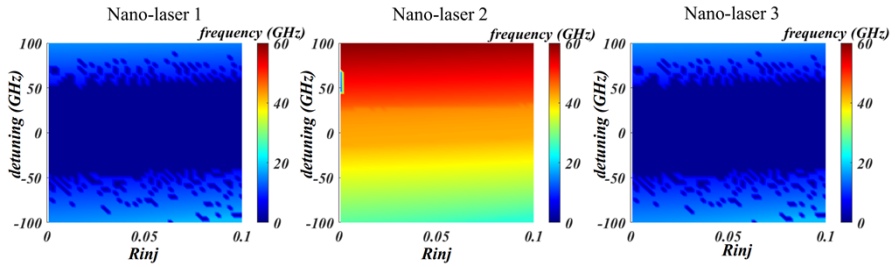

Fig. 8. Distribution of the oscillation frequency of nano-lasers in the second scenario of the nano-laser array with optical injection shown in Fig. 1(b) when α=2 and the coupling rate $k_{12} = k_{23} = 5 \times 10^9$. The modulation frequency and the modulation depth of the master laser are set to be 25 GHz and 0.1 respectively.

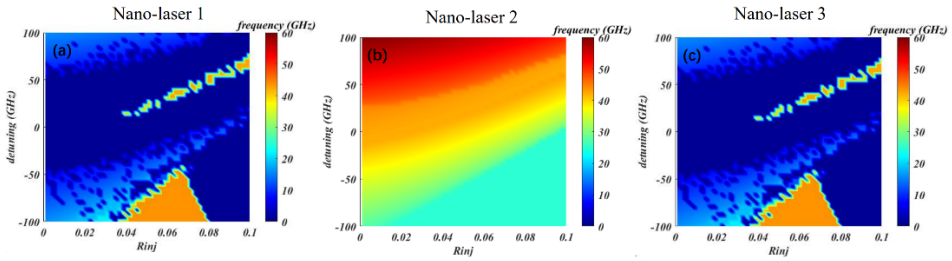

Fig. 9. Distribution of the oscillation frequency of nano-lasers in the second scenario of the nano-laser array with optical injection shown in Fig. 1(b) when α=2 and the coupling rate $k_{12} = k_{23} = 5 \times 10^9$. The modulation frequency and the modulation depth of the master laser are set to be 25 GHz and 0.3 respectively.

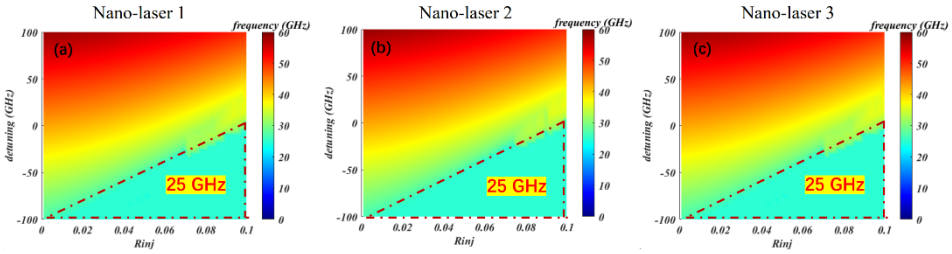

Fig. 10. Distribution of the oscillation frequency of nano-lasers in the third scenario of the nano-laser array with optical injection shown in Fig. 1(c) when α=2 and the coupling rate $k_{12} = k_{23} = 5 \times 10^9$. The modulation frequency and the modulation depth of the three master lasers are set to be 25 GHz and 0.3 respectively.

The value of the induced oscillation frequency is determined primarily by the modulation frequency and the frequency detuning. However, the precise relationship between the induced oscillation frequency and the detuning is also determined by the strength of the optical injection and the modulation depth. Further exploration of this relationship will be made in future work.

As an illustration of many possible variations on this theme, in Fig. 11 consideration is given to the case where the slave lasers are subjected to modulated optical injection at different modulation frequencies: 10 GHz for nano-laser 1; 25 GHz for nano-laser 2 and 35 GHz for nano-laser 3. Clearly there is no expectation of symmetry in the responses of nano-lasers 1 and 3 in this case.

Optics EXPRESS

In general the 2D portraits show zones of various oscillations frequencies with the signature of the modulation frequencies of the master lasers being apparent in all cases.

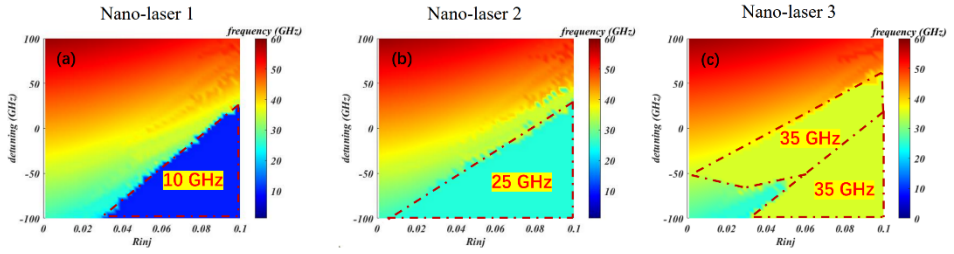

Fig. 11. Distribution of the oscillation frequency of nano-lasers in the third scenario of the nano-laser array with optical injection shown in Fig. 1(c) when α=2 and the coupling rate $k_{12} = k_{23} = 5 \times 10^9$. The modulation frequency of the three master lasers are set to be 10 GHz, 25 GHz and 35 GHz respectively for nano-laser 1-3. The modulation depth of the three master lasers are set to be 0.3.

4. Conclusion

This initial study of the optical injection response of a small array of electrically pumped nano-laser arrays has shown that a wide range of dynamical behaviours can be excited by continuous wave and modulated optical injection. Bifurcation diagrams have been presented for both cases. In the case of continuous wave optical injection, it has been shown that several forms of periodic dynamics arise as well as quasi-periodic and chaotic dynamics. Characteristic frequencies of the dynamics are related to the 23 GHz resonance frequency of stand-alone nano-lasers whilst a 43 GHz feature appears to arise due to auto-modulation of the nano-lasers. For the case of modulated optical injection, it is shown that bands of high-frequency oscillations are induced as the detuning between the master and slave laser and the strength of the optical injection is increased. It has been indicated that there is a nuanced dependence of the induced oscillation frequency on the modulation frequency and the detuning frequency. Further work will be undertaken to clarify this dependence. It is apparent that there are many other options which can be considered with a view to seeking specific responses in nano-laser arrays when subject to optical injection. Alternative array geometries may be a fruitful area in which to seek other behaviours. It is intended to investigate some of those options in future work. In addition, it is planned to relax the assumption that all elements of the array are identical so that the impact of device variation on the dynamical behaviour can be assessed.

Funding. Fundamental Research Funds for the Central Universities (XJSJ24087); Proof of Concept Foundation of Xidian University Hangzhou Institute of Technology (GNYZ2023QC0402).

Disclosures. The authors declare no conflicts of interest.

Data availability. Data underlying the results presented in this paper are not publicly available at this time but may be obtained from the authors upon reasonable request.

References

1. C. Z. Ning, "Semiconductor Nano-lasers: Semiconductor Nano-lasers," Phys. Stat. Sol. (b) **247**(4), 774–788 (2010).
2. D. Saxena, S. Mokkapati, and C. Jagadish, "Semiconductor Nano-lasers," IEEE Photonics J. **4**(2), 582–585 (2012).
3. Q. Gu and Y. Fainman, *Semiconductor Nano-lasers*. Cambridge: Cambridge University Press, 2017.
4. R.-M. Ma and R. F. Oulton, "Applications of Nano-lasers," Nat. Nanotech. **14**(1), 12–22 (2019).
5. M. P. Nezhad, A. Simic, O. Bondarenko, *et al.*, "Room-Temperature Subwavelength Metallo-Dielectric Lasers," Nat. Photonics **4**(6), 395–399 (2010).
6. Y. Hou, P. Renwick, B. Liu, *et al.*, "Room Temperature Plasmonic Lasing in a Continuous Wave Operation Mode from an InGaN/GaN Single Nanorod with a Low Threshold," Sci. Rep. **4**(1), 5014 (2014).

Optics EXPRESS

7. C. Li, J. B. Wright, S. Liu, *et al.*, "Nonpolar InGaN/GaN Core-Shell Single Nanowire Lasers," Nano Lett. **17**(2), 1049–1055 (2017).
8. D. I. Song, A. Yu, P. Samutpraphoot, *et al.*, "Three-Dimensional Programming of Nano-laser Arrays through a Single Optical Microfiber," Optica **9**(12), 1424–1432 (2022).
9. M. T. Hill, Y.-S. Oei, B. Smalbrugge, *et al.*, "Lasing in Metallic-Coated Nanocavities," Nat. Photonics **1**(10), 589–594 (2007).
10. J. H. Lee, M. Khajavikhan, A. Simic, *et al.*, "Electrically Pumped Sub-Wavelength Metallo-Dielectric Pedestal Pillar Lasers," Opt. Express **19**(22), 21524 (2011).
11. K. Ding, Z. C. Liu, L. J. Yin, *et al.*, "Room-Temperature Continuous Wave Lasing in Deep-Subwavelength Metallic Cavities under Electrical Injection," Phys. Rev. B **85**(4), 041301 (2012).
12. K. Ding, M. T. Hill, Z. C. Liu, *et al.*, "Record Performance of Electrical Injection Sub-Wavelength Metallic-Cavity Semiconductor Lasers at Room Temperature," Opt. Express **21**(4), 4728 (2013).
13. K. H. Li, X. Liu, Q. Wang, *et al.*, "Ultralow-Threshold Electrically Injected AlGaN Nanowire Ultraviolet Lasers on Si Operating at Low Temperature," Nat. Nanotech. **10**(2), 140–144 (2015).
14. K. Ren, C. Li, Z. Fang, *et al.*, "Recent Developments of Electrically Pumped Nano-lasers," Laser Photonics Rev. **17**(5), 2200758 (2023).
15. M. Lorke, T. Suhr, N. Gregersen, *et al.*, "Theory of Nano-laser Devices: Rate Equation Analysis versus Microscopic Theory," Phys. Rev. B **87**(20), 205310 (2013).
16. B. Romeira and A. Fiore, "Purcell Effect in the Stimulated and Spontaneous Emission Rates of Nanoscale Semiconductor Lasers," IEEE J. Quantum Electron. **54**(2), 1–12 (2018).
17. Y. Fan, Y. Hong, and P. Li, "Numerical Investigation on Feedback Insensitivity in Semiconductor Nano-lasers," IEEE J. Select. Topics Quantum Electron. **25**(6), 1–7 (2019).
18. Z. Sattar and K. A. Shore, "Analysis of the Direct Modulation Response of Nanowire Lasers," J. Lightwave Technol. **33**(14), 3028–3033 (2015).>
19. P. Jiang, P. Zhou, N. Li, *et al.*, "Optically Injected Nano-lasers for Time-Delay Signature Suppression and Communications," Opt. Express **28**(18), 26421 (2020).
20. T. S. Rasmussen and J. Mork, "Theory of Microscopic Semiconductor Lasers with External Optical Feedback," Opt. Express **29**(10), 14182 (2021).
21. Z. Abdul Sattar and K. A. Shore, "Phase Conjugate Feedback Effects in Nano-Lasers," IEEE J. Quantum Electron. **52**(4), 1–8 (2016).
22. H. Han and K. A. Shore, "Dynamics and Stability of Mutually Coupled Nano-Lasers," IEEE J. Quantum Electron. **52**(11), 1–6 (2016).
23. S. S. Deka, S. Jiang, S. H. Pan, *et al.*, "Nano-laser Arrays: Toward Application-Driven Dense Integration," Nanophotonics **10**(1), 149–169 (2020).
24. Y. Fan, K. A. Shore, and X. Shao, "Dynamics of electrically-pumped semicondcutor nano-laser arrays," Photonics **10**(11), 1249 (2023).
25. Y. Fan, S. An, K. A. Shore, *et al.*, "Tailoring the direct current modulation response of electrically-pumped semiconductor nano-laser arrays," Photonics **10**(12), 1373 (2023).
26. Z. A. Sattar and K. A. Shore, "External optical feedback effect in semiconductor nano-lasers," IEEE J. Select. Topics Quantum Electron. **21**(6), 500–505 (2015).
27. V. Annovazzi-Lodi and S. Donati, "Injection modulation in coupled laser oscillators," IEEE J. Quantum Electron. **16**(8), 859–864 (1980).
28. V. Annovazzi-Lodi, S. Donati, and M. Manna, "Chaos and locking in a semiconductor laser due to external injection," IEEE J. Quantum Electron. **30**(7), 1537–1541 (1994).